Available online at www.eccomasproceedia.org
Eccomas Proceedia COMPDYN (2023) 3064-3076

ECCOMAS
Proceedia

COMPDYN 2023
9th ECCOMAS Thematic Conference on
Computational Methods in Structural Dynamics and Earthquake Engineering
M. Papadrakakis, M. Fragiadakis (eds.)
Athens, Greece, 12-14 June 2023

ANALYSIS OF THE FORCE RESPONSE OF BEARING DEVICES FOR BRIDGE STRUCTURES

Marco Furinghetti[1,2], Simone Reale[1], Matt J. Fox[1], Yuan Fan[1], Chiara Casarotti[2], and Alberto Pavese[1]

[1] University of Pavia
via Ferrata 3, 27100 Pavia (Italy)
e-mail: marco.furinghetti@unipv.it, simone.reale01@universitadipavia.it, yuan.fan@unipv.it, matt.fox@unipv.it, a.pavese@unipv.it

[2] EUCENTRE Foundation
via Ferrata 1, 27100 Pavia (Italy)
marco.furinghetti@eucentre.it, chiara.casarotti@eucentre.it

Abstract

Bridge structural systems are often represented by high risk levels, from several standpoints. The strategic role they generally play in the infrastructure network leads to significant exposure characteristics, with a resulting high risk level. Even though the seismic action is not always a key issue for a considered bridge, excessive horizontal loading may lead to unexpected failures at specific local levels. Among all the possible structural elements, bearing devices can represent in some case the most vulnerable component of the overall system, which can cause sudden and brittle collapses, at ultimate conditions. In this work the behavior of bearing devices for bridge structural systems has been analyzed, by comparing the outcomes of experimental campaigns to numerical parameters, commonly adopted in analytical simulations. Then, some case study structures have been modeled, in order to carry out a parametric study, with varying mechanical properties, and consequently accounting for the effect of aging on the force response of the single devices. Special attention has been focused on the displacement at the bearing locations, rather than the internal forces of piers, and results have been normalized with respect to the mean values for the assumed mechanical properties.

Keywords: Bridge, Reinforce Concrete, Bearing Devices, Experimental Campaign, Parametric Study.

ISSN:2623-3347 © 2023 The Authors. Published by Eccomas Proceedia.
Peer-review under responsibility of the organizing committee of COMPDYN 2023.
doi: 10.7712/120123.10623.21210

1 INTRODUCTION

Bridge structural systems present several facets that need to be discussed to properly understand the structural response under different actions. Bridges generally play a strategic role in infrastructure networks, which leads to significant exposure characteristics and to a resulting high risk level.

The seismic action, which is not always a key issue for bridge structures, can lead to significant damage in the structural elements, with effects on the response of the whole bridge. The effects of multiple earthquakes on a bridge structure can reduce its seismic reliability [1]. The effects of aftershocks on the seismic response of bridges have been studied by Pang and Wu [2]. The study considered reinforced concrete continuous bridges, highlighting that aftershock events can increase the system fragility, the displacement of the bearings and the curvature of piers. Many existing bridges have been designed, when there were not specific requirements in terms of structural details. In such situation, it is reported that the fragility of the joints highly influences the seismic vulnerability of the whole structure [3].

Considering the case of the Italian road network, most of the bridges have been built around the middle of the last century and have reached or exceed their design life. The degradation in the properties of bridges has played a key role in some collapse events that occurred in recent years [4]. The rise in frequency of bridge collapses is a clear indicator of the effects of aging, with eventual lack of maintenance [5]. Proper maintenance is fundamental, since the most important element in the durability of bridges is the correct evolution of the structure within the design lifetime. Critical points of structures (especially for reinforced concrete bridges in particular) are not always easy to detect. Among all the possible structural elements, bearing devices can represent in some case the most vulnerable component of the overall system, causing sudden and brittle collapses, at ultimate conditions.

To properly assess the effects of aging on the materials, it is necessary to consider both experimental and numerical results. In particular, this work analyzes the behavior of bearing devices for bridge structural systems, comparing the outcomes of experimental campaigns to numerical parameters. A parametric study has been then carried out, in order to investigate the effect of aging on the response of bearing devices, focusing on displacements undergone by the device and on actions transmitted to the piers.

2 EXPERIMENTAL OUTCOMES ON FULL-SCALE DEVICES

In Figure 1 the specimens under investigation are shown.

a) b)

Figure 1: Full-scale *new generation* (a) and *naturally aged* (b) elastomeric bearings.

Full-scale bearing devices have been experimentally tested at the Laboratory of EUCENTRE Foundation in Italy, in order to assess the characteristics of the force response of elastomeric bearings, used for bridge structural systems in the last decades. Specifically, the plan sizes are 700mm and 350mm, with an average thickness of 35mm. The naturally aged bearings consist of dismissed devices, which were previously installed into an existing bridge structural system. Thus, the presented testing campaign can be considered as an evidence of the mechanical properties of commonly adopted elastomeric bearing devices, in agreement with the material properties used in the last 50 years.

2.1 Testing protocol

The testing protocol to be applied to the aforementioned devices has been defined, according to the European Standard Code for Bearing Devices, UNI:EN1337, and all tests are summarized in Table 1.

Table 1: Testing protocol for full-scale bearing devices.

test #	test name	label	main dof	Ampl.	Max. vel.	Freq.	load shape	Vert. load [kN]	Cycles [#]
1	Shear Stiffness at ambient temperature	SS	long	± 100%	3 mm/s	0.016 Hz	triangular	1470	2
2	Shear bond at ambient temperature	SB	long	± 200%	2 mm/s	0.007 Hz	triangular	2940	2
3	Compression stiffness	CS	vert	-	24.5 kN/s	-	loading ramp	2940	3
4	Static rotation eccentricity method	SR	vert	0.470 deg	-	-	loading ramp	1715	2
5	Static rotation restoring moment	SR	vert	0.172 deg	-	0.030 Hz	triangular	1715	10

In this work the analysis of the experimental outcomes of tests #1 and #2 are discussed, since the force response of the bearings is under investigation. Both tests are related to low-velocity longitudinal tests, performed by applying a triangular displacement waveform, with 100% and 200% of peak shear strain respectively for Shear Stiffness and Shear Bond tests. The vertical load is kept as constant during the whole duration of the tests, in order to simultaneously apply compression and shear states of stress.

2.2 Testing setup

All tests have been performed at the Laboratory of EUCENTRE Foundation in Italy, through the Bearing Tester System (BTS). Such a testing equipment is capable of performing static and dynamic tests on full-scale bearing and isolation devices, thanks to large displacement and force capacity levels for both longitudinal and vertical directions. In Figure 2 the testing equipment is shown.

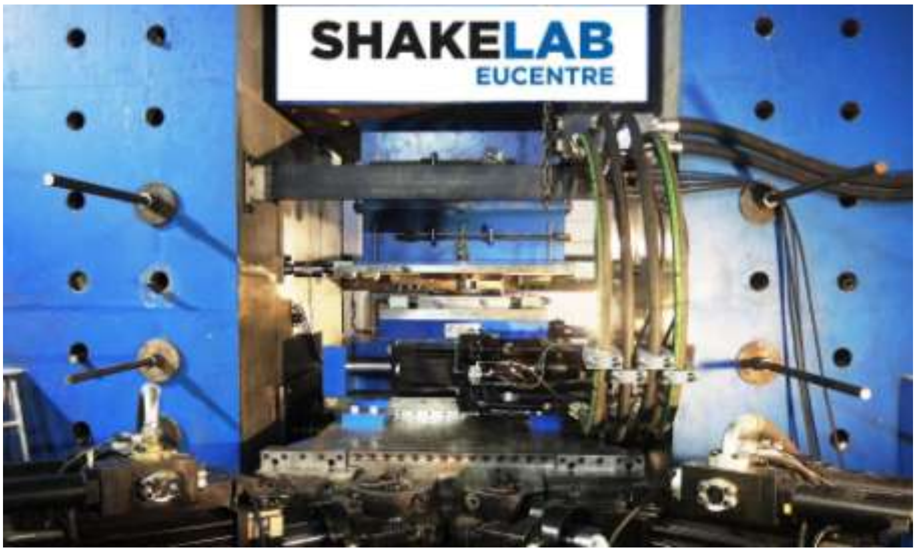

Figure 2: Bearing Tester System at EUCENTRE Foundation (Italy).

Since bearing devices are commonly tested just laid on the setup backing plates, by considering just a frictional coupling between the testing equipment and the bearings, special steel plates have been designed and installed, in order to ensure the correct application of the horizontal motion, without eventual sliding induced by high forces. To this aim, the roughness of the interfaces between bearings and testing equipment has been increased, through mechanical the realization of grooves, which allows to better apply horizontal displacements, with no sliding motions, which would result into small portion with constant horizontal force within the hysteretic loops.

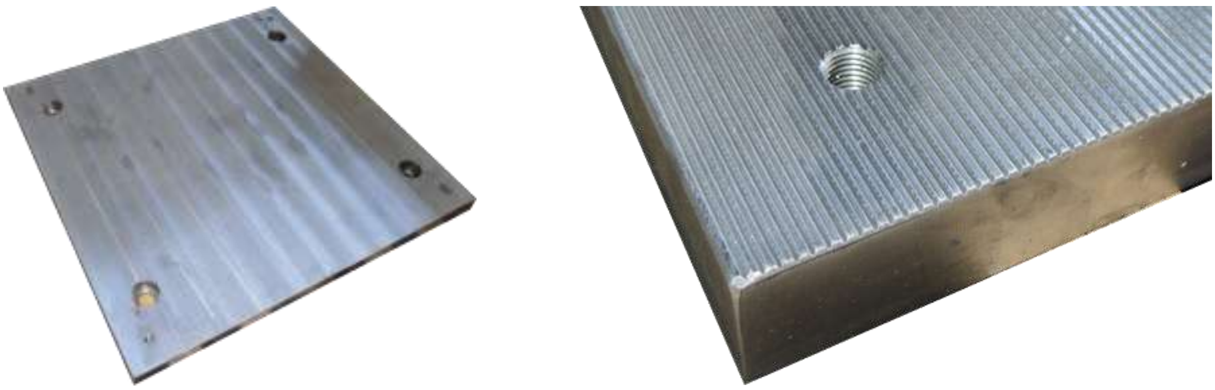

Figure 3: Backing plates for effective application of motion.

Consequently, the resulting mechanical properties of the devices can be correctly evaluated, since the effective hysteretic response of the devices is returned by the proper application of test horizontal motion.

2.3 Test results

In what follows testing results are analyzed. More specifically, hysteretic response is discussed, in addition to the shear modulus obtained as a function of the effective stiffness at maximum displacement, together with the equivalent viscous damping.

In Figure 4 the hysteretic loops are shown, for one new and one aged devices.

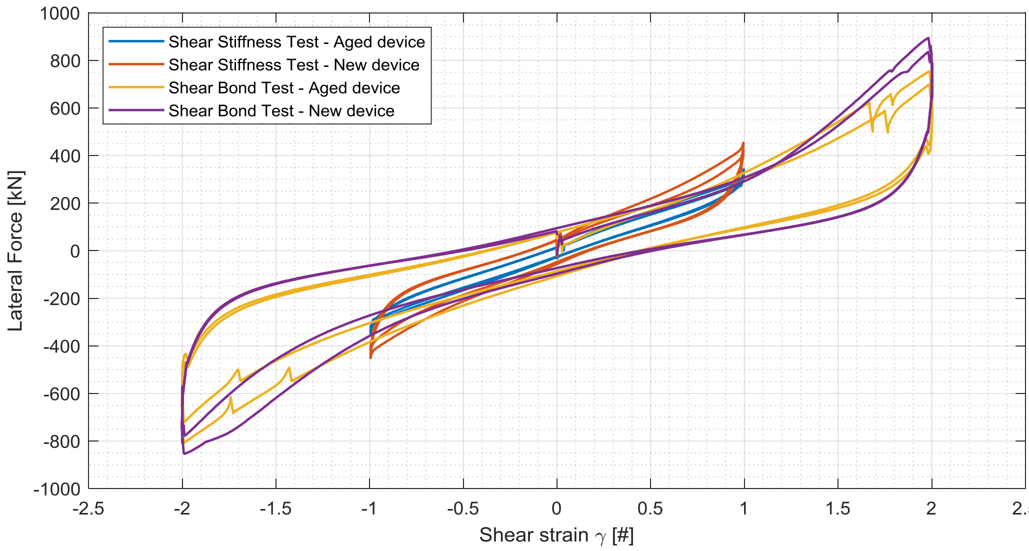

Figure 4: Example of hysteretic loops for both aged and new bearing devices.

As can be noted, the behavior of the bearings can be considered approximately linear elastic, with a certain value of equivalent viscous damping, as the lateral shear strain does not exceed 100%. For tests at 200% of shear strain, the hysteresis area significantly increases, together with a considerable hardening, which may result into increased values of both equivalent shear modulus and viscous damping.

In Figure 5 values of the equivalent shear modulus G are reported, obtained as a function of the effective stiffness at maximum displacement, by considering *Shear Stiffness* tests.

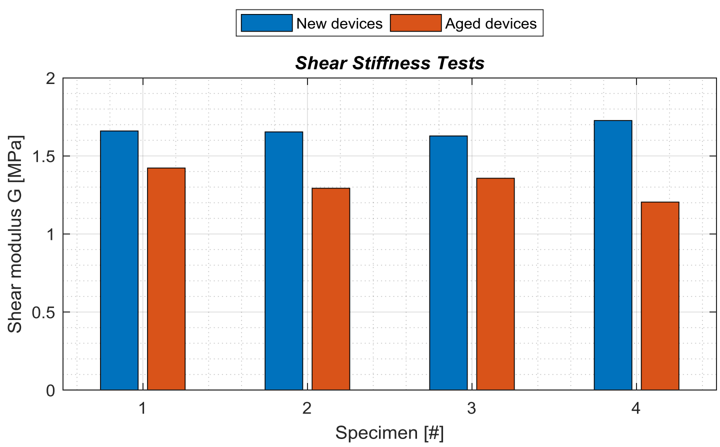

Figure 5: Equivalent shear modulus for *Shear Stiffness* tests.

Graphical results for the shear modulus at 100% shear strain show that the new compound has a higher shear modulus, in comparison to the naturally aged devices, for all specimens. However, since details of the original design value of the dismissed bearings are missing, it is not possible to directly address such differences to the aging effect, rather that possible discrepancies in the compound characteristics. On the other hand, it is possible to assess a range of variation of the shear modulus for elastomeric bearings, to be implemented in real practice applications of bridge structural systems.

Finally, in Figure 6 experimental results are reported, as equivalent viscous damping values.

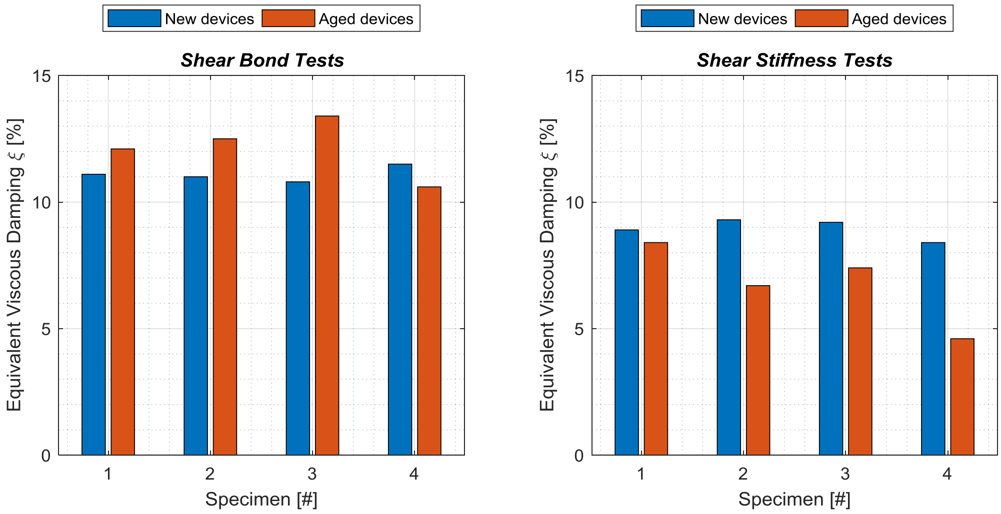

Figure 6: Equivalent Viscous Damping for *Shear Bond* and *Shear Stiffness* tests.

As previously discussed, tests with 200% of peak shear strain have larger values of damping ratios, due to the larger hysteresis area, in comparison to tests with 100% of shear strain. Concerning the comparison between naturally aged and new devices, it is not possible to detect a common trend, since damping results are higher for aged bearings at 200% of shear strain, and the opposite behavior can be noticed at 100% of shear strain. In addition, as the displacement demand does not exceed 100% of shear strain, the equivalent viscous damping, as expected, is quite low (between 5% and 10%), and consequently a lower bound of 5% damping is recommended, when no sufficient information about the compound mechanical properties are available.

3 ASSESSMENT OF CASE STUDY STRUCTURES

Two case study structures have been modeled, in order to perform a parametric study, by considering the effects of aging on the force and displacement responses of elastomeric bearing devices.

Bridge #1 is located in a region associated to low seismic hazard. The bridge is characterized by three simply supported spans. The total length of Bridge #1 is 44 m. The width of the deck is 16.5 m, with two carriageways, divided by a fixed traffic divider. The deck is composed of 14 prestressed concrete beams with I-shape section. The height of the beams is 1.3 m in the central span and 0.9 m in the lateral spans. Transversal reinforced concrete beams, used as stiffeners, are present along the deck, which is completed by an upper slab 0.25m thick. A neoprene pad bearing is present below each beam. Six lines of devices have been identified. Each device is 3 cm high, with plan dimensions of 0.4 x 0.35 m. Each of the two piers of Bridge #1 is made up of four columns topped by an L-shaped pier cap. The columns present a square section with side 0.8 m. Shallow foundations are present below the piers. In particular, a continuous footing with section 2 x 1 m has been identified and modeled below each piers. No detailed information were available for the abutments, which have been modeled in a simplified way. The mechanical properties of the materials employed in the model have been defined, by considering the results of experimental tests.

On the other hand, the construction site of Bridge #2 is associated to a high seismic hazard. Four simply supported 12.5 m long spans characterize the case study. The total length of the bridge is 50 m. The width of the deck is 10.5 m. The carriageway is divided into two lanes (one for each direction of travel). The deck is composed of 5 reinforced concrete beams with section 0.4 x 0.95 m. Transversal reinforced concrete beams, used as stiffeners, are present along the deck. The deck is completed by a 0.3 m thick upper slab. A neoprene pad bearing is present below each beam. Eight lines of devices have been identified. Each device is 2.5 cm high, with plan dimensions of 0.4 x 0.6 m. Bridge #2 presents three piers with frame structure. In each pier, two columns with section 1.2 x 1 m are topped by a pier cap with section 1.3 x 1.25 m. The foundations of piers and abutments consist of piles with 1.2 m diameter. The data required to define the mechanical properties of the materials employed in the model have been obtained considering the results of experimental tests on the structure.

Figure 7 presents the FEM models developed to perform the parametric study on the two case studies. The models have been developed by using SAP2000 [6]. Longitudinal and transverse beams, columns, pier caps and continuous footing have been modeled using beam elements. The bearings have been modeled using two nodes link elements, assigning to each degree of freedom the corresponding stiffness to properly characterize the devices. The upper slab of the deck of each bridge has been modeled using Shell elements. This procedure was necessary to properly capture the response of the deck, as a result of the load configurations considered in this study. Given their inherently two-dimensional nature, abutments have also been model using Shell elements.

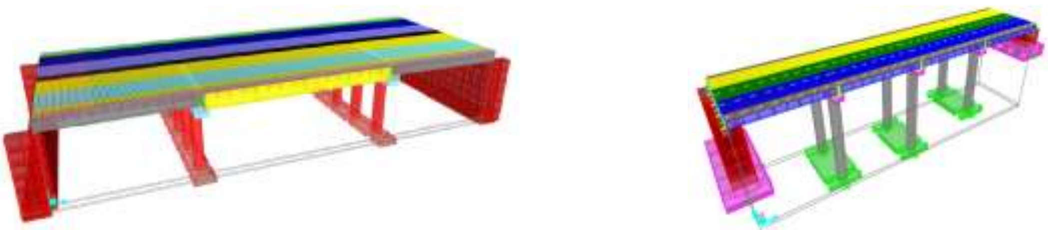

a) b)

Figure 7: Case study structures FEM models with low (Bridge #1 - a) and high (Bridge #2 - b) seismic hazard.

As briefly aforementioned, the two case studies have been considered in a parametric study with the aim of investigating the effects of aging in the variation of the mechanical properties of bearings, and the consequent modifications in the overall structural response, subjected to both ordinary and seismic loads.

As reported in the scientific literature, one of the possible modifications in the properties of the bearings due to aging effects is the increase or reduction of their stiffness [7][8]. Thus, a wide range of variation of the mechanical properties of elastomeric bearings has been considered in the presented parametric study.

The parametric study has been carried out by performing linear dynamic analyses in SAP2000. For each case study, 11 models have been defined. Each model was characterized by a different value of horizontal stiffness of the bearings K_h, which is computed as follows:

$$K_h=GA/h \tag{1}$$

Where G is the shear modulus of the rubber compound, A is the plan area of the device and h is the total height of all the elastomeric layers.

Particularly, the bearing properties have been obtained, by varying the value of G between 0.5MPa and 1.5MPa. Once the linear dynamic analyses have been completed, the obtained results have been processed to define the variation of the considered response parameters with the value of G.

In order to summarize the procedure adopted for the parametric study, four main steps can be identified:

- Definition of the models of the case studies;
- Load analysis;
- Linear dynamic analyses for different values of G;
- Post-processing of the results.

3.1 Load configurations and combinations

To properly introduce the analysis of results returned by the parametric study, the description of the adopted configurations and combinations considered in the study is of fundamental importance. The following actions have been considered for both the case studies:

- Structural dead loads;
- Non-structural dead loads;
- Snow;
- Traffic loads (including the braking force);
- Seismic action.

The wind action has not been considered in the present study, since is not considered as a significant contribution. The Italian Building Code (NTC2018 [9]) represented the main reference in the definition of the acting loads. Structural dead loads have been automatically computed by the software, while a typical configuration of the roadway finishes has been considered, for the definition of the non-structural dead loads. The snow load has been defined considering the prescriptions of §3.4 of NTC2018. The seismic load has been defined as horizontal and vertical response spectra, corresponding to the Life-Safety and Damage Limit States, in agreement with NTC2018.

The definition of the traffic loads requires some specific considerations for both the case studies. Figure 8 represents the lane definition for Bridge #1 and Bridge #2. Both the case studies are road bridges, thus the traffic loads in the vertical direction are defined considering the Scheme 1, as ruled by NTC2018. The definition of the traffic loads is needed to identify the lanes. Given the configuration of Bridge #1, four 3 m wide lanes (two for each traffic direction) have been identified, whereas Bridge #2, has three 3 m wide lanes.

In the definition of the traffic loads, the braking force has been taken into account. The braking force is defined as a percentage of the vertical traffic load and is applied in horizontal direction, along the traffic direction.

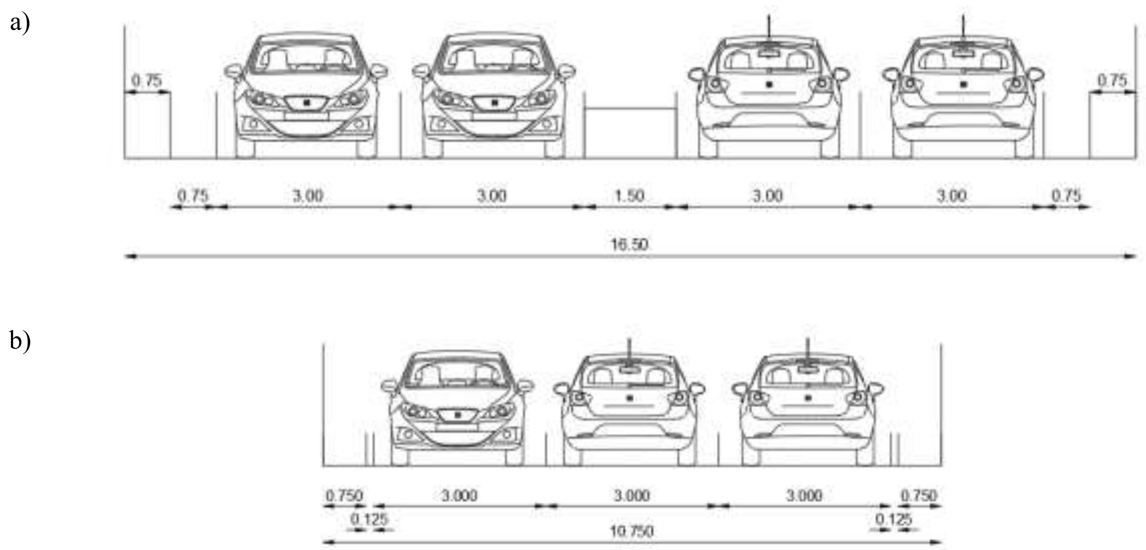

Figure 8: Lane definition for the traffic load computation: Bridge #1 (a) and Bridge #2 (b).

The parametric study required the definition of load combinations for static and seismic conditions. In both cases, the combinations have been defined following the prescriptions of NTC2018. Specific considerations are required in the definition of the static load combinations.

For static load combinations, the traffic loads must be defined with different configurations, in order to maximize the response of the structure. To this aim, six different configurations of the traffic lanes defined according to the NTC2018 have been considered for both the case study structures. The influence of the moving loads has been taken into account in the study, by employing the tandem loads defined in the NTC2018. For each span, three different positions (the two ends and the middle of the span) of the moving loads have been considered in order to maximize the structural response.

Figure 9 represents a scheme of the traffic load configurations for Bridge #1 and Bridge #2.

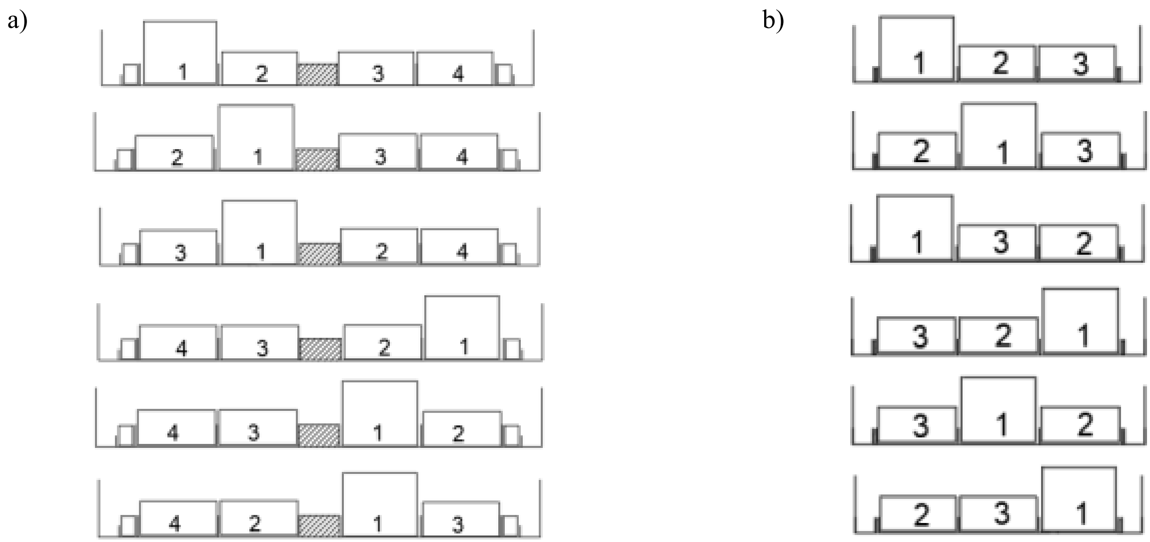

Figure 9: Traffic load configurations: Bridge #1 (a) and Bridge #2 (b).

3.2 Analysis of results

In this section the analysis of the results of the parametric study introduced earlier is presented. In the post-processing of results special attention has been focused on the horizontal displacements of the bearings, the shear force transmitted to the piers and the bending moment transmitted to the piers. Peak values of each response quantity have been normalized with respect to corresponding value returned by considering a shear modulus G equal to 1 MPa.

Figure 10 reports the displacement ratio for one line of bearings of Bridge #1 and Bridge #2. For each value of G and considering all the different load combinations, the maximum value of displacement in a given line of bearings in both longitudinal and transverse direction has been taken and successively normalized with respect to the value of displacement in the same direction, returned by considering the shear modulus G equal to 1 MPa. It has to be pointed out that U_2 is the displacement in the longitudinal direction of the bridge, while U_3 refers to the transverse direction.

Considering all the bearing lines, maximum peak displacements, for both the case studies, have been detected at the abutments locations. It can be noted that the displacement demands decrease with the increase of G, since the horizontal stiffness of the bearings increases. As expected, results provide evidence that the shear modulus G has a significant influence on the peak horizontal displacements of the bearings and that aging phenomena are relevant in this sense. Significant variations have been computed, bounded between -15% and 35%.

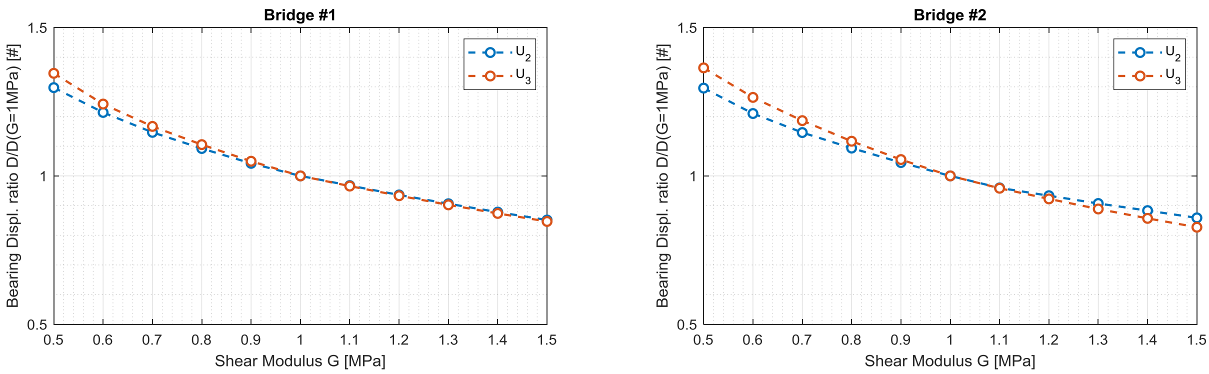

Figure 10: Numerical results: Displacement ratio for Bridge #1 (left) and Bridge #2 (right).

Figure 11 shows the results in terms of shear ratio for both the case studies. Data have been processed similarly to what has been done for the bearings' peak displacement demand. For each pier, the peak value of shear force transmitted to the columns has been identified, by considering all the load combinations, and results have been normalized with respect to the value corresponding to a shear modulus G equal to 1 MPa. V_{22} indicates the shear in the plane parallel to the longitudinal direction of the bridge, while V_{33} refers to the shear in the plane perpendicular to the longitudinal direction of the bridge.

Figure 12 is related to the bending moment ratio for Bridge #1 and Bridge #2. The post-processing of the data obtained with the analyses is almost equal to the procedure employed to derive the shear ratio. M_{22} represents the moment acting in the plane perpendicular to the bridge longitudinal axis, while M_{33} indicates the moment in the plane parallel to the bridge longitudinal axis.

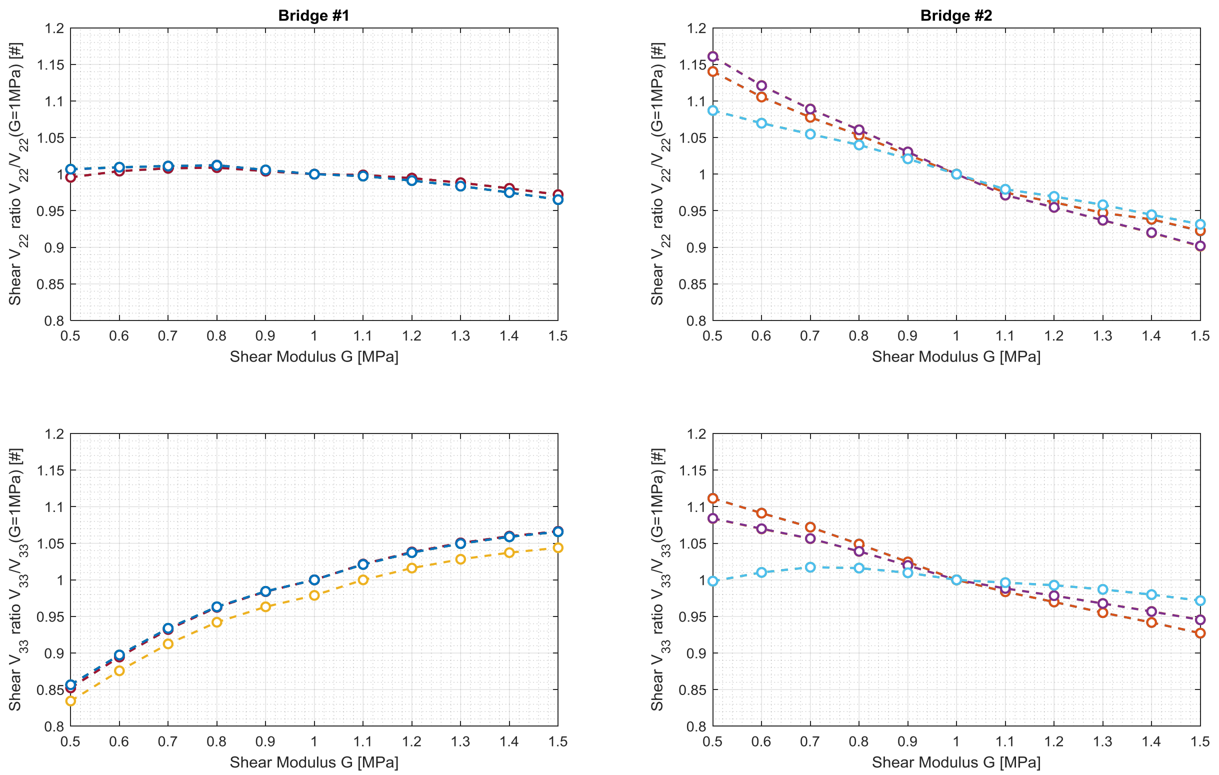

Figure 11: Numerical results: Shear ratio for Bridge #1 (left) and Bridge #2 (right).

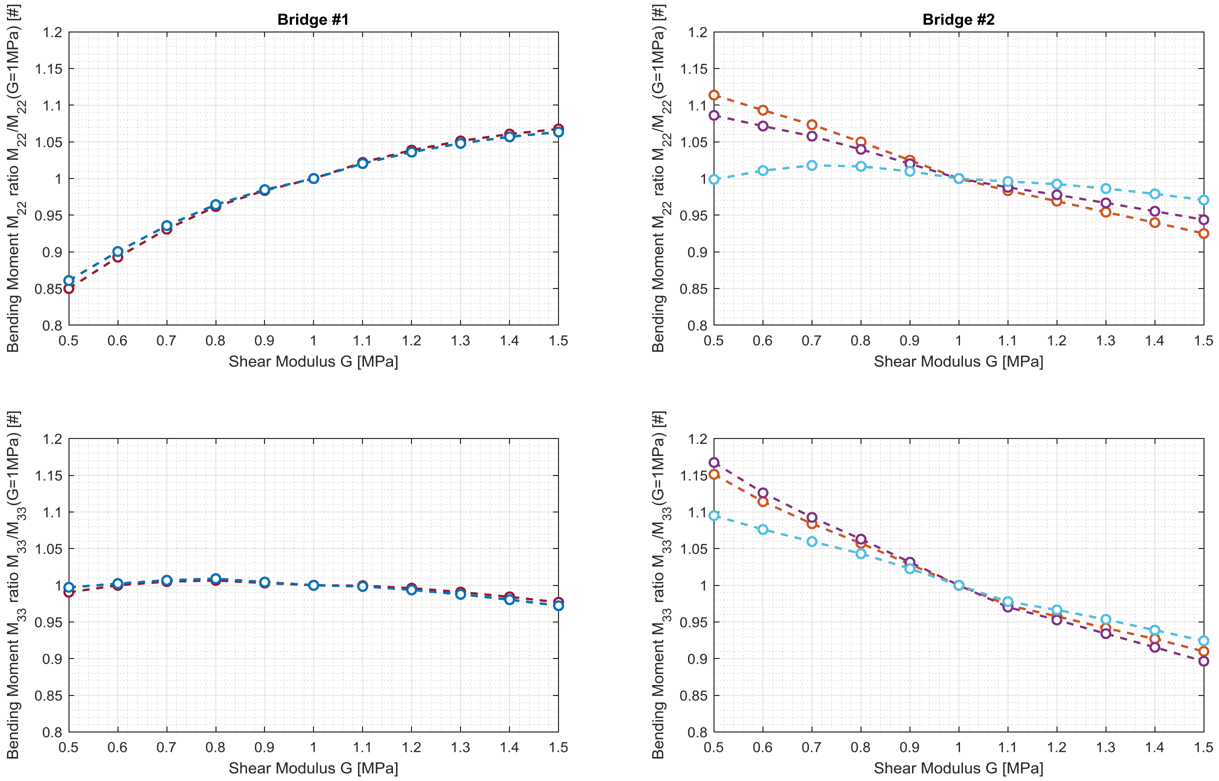

Figure 12: Numerical results: Bending Moment ratio for Bridge #1 (left) and Bridge #2 (right).

Considering Bridge #1, it can be noticed that the variation for V_{22} is relatively small, while for V_{33} values become more relevant (around 15% for values of G below 1 MPa, and approximately 6% for values of G greater than 1 MPa). Similar results can be observed in terms of bending moments, with M_{22} exhibiting greater variations compared to M_{33}.

Considering the case of Bridge #2, for V_{22} the variation is around 10% for values of G greater than 1 MPa and around 15% when G is less than 1 MPa. In the case of V_{33}, the variation is 10% for G less than 1 MPa and 8% when G is greater than 1 MPa. Similar results can be observed considering the moments M_{22} and M_{33}.

The parametric study that has been carried out allows to understand how the aging effects on bearing devices can modify the actions transmitted to the piers. It has to be remarked, however, that the study considers only two case studies and that an extended sample of bridges could be useful to better generalize the drawn conclusions.

4 CONCLUSIONS AND FUTURE DEVELOPMENTS

The presented research show the outcomes of both experimental and numerical campaigns, with the aim of analyzing the characteristics of the force response of elastomeric bearings for bridge structural systems, and the influence of the mechanical properties of the adopted rubber compound on the overall response. The results have shown the following issues:

- Naturally aged devices seems to have a lower stiffness, in comparison to new generation bearings;
- On the other hand, it is not possible to detect a general trend for the equivalent viscous damping, since is seems to be significantly affected by the hardening and increase of hysteresis area for shear strains higher of 100%.
- The shear modulus variation leads to non-negligible variations in the displacement demand of the deck, as well as for shear and bending moment peak responses.

As a future development of this endeavor, the new generation devices will be artificially aged through a special procedure which implies a certain duration of high temperature application to the bearings, in order to better distinguish the effects of aging on the mechanical properties of the adopted rubber compound.

ACKNOWLEDGEMENT

This work was funded by the agreement between the Italian Consiglio Superiore dei Lavori Pubblici and the ReLUIS Consortium on "Sperimentazione delle linee guida per la classificazione e gestione del rischio, la valutazione della sicurezza ed il monitoraggio dei ponti esistenti", Decreto del Ministero delle Infrastrutture n. 578 del 17.12.2020.

REFERENCES

[1] Kumar R, Gardoni P. Effect of seismic degradation on the fragility of reinforced concrete bridges. Eng Struct 2014;79:267–75. https://doi.org/10.1016/j.engstruct.2014.08.019.

[2] Pang Y, Wu L. Seismic Fragility Analysis of Multispan Reinforced Concrete Bridges Using Mainshock-Aftershock Sequences. Math Probl Eng 2018;2018:1–12. https://doi.org/10.1155/2018/1537301.

[3] Taghinia A, Vasseghi A, Khanmohammadi M, Soroushian A. Development of Seismic Fragility Functions for Typical Iranian Multi-Span RC Bridges with Deficient Cap Beam–Column Joints. International Journal of Civil Engineering 2022;20:305–21. https://doi.org/10.1007/s40999-021-00661-5.

[4] Fox MJ, Furinghetti M, Pavese A. Application of the new Italian assessment guidelines to a 1960s prestressed concrete road bridge. Structural Concrete. 2022. https://doi.org/10.1002/suco.202200884

[5] Cosenza E, Losanno D. Assessment of existing reinforcedconcrete bridges under road-traffic loads according to the new Italian guidelines. Structural Concrete 2021;22:2868–81. https://doi.org/10.1002/suco.202100147.

[6] CSI, “SAP2000 Integrated Software for Structural Analysis and Design,” Computers and Structures Inc., Berkeley, California.

[7] Itoh, Y., and H. S. Gu. "Prediction of aging characteristics in natural rubber bearings used in bridges." *Journal of Bridge Engineering* 14.2, 2009.

[8] Oh, Ju, Jin Ho Kim, and Hwa Cho Yi. "Effects of thermal aging of laminated rubber bearing on seismic performance of bridges." *Journal of Vibroengineering* 18.6, 2016

[9] Norme Tecniche per le Costruzioni. Aggiornamento delle Norme tecniche per le costruzioni. Gazzetta Ufficiale Serie Generale 2018;42.